NANO LETTERS

2007
Vol. 7, No. 2
394−397

Fast, Ultrasensitive Virus Detection Using a Young Interferometer Sensor

Aurel Ymeti,*,† Jan Greve,† Paul V. Lambeck,‡ Thijs Wink,§ Stephan W.F.M. van Hövell,§,# Tom A.M. Beumer,|| Robert R. Wijn,⊥ Rene G. Heideman,⊥ Vinod Subramaniam,† and Johannes S. Kanger†

Biophysical Engineering, MESA+ Institute for Nanotechnology and Institute for Biomedical Technology, University of Twente, PO Box 217, 7500 AE Enschede, The Netherlands, Integrated Optical Microsystems, MESA+ Institute for Nanotechnology, University of Twente, PO Box 217, 7500 AE Enschede, The Netherlands, Paradocs Group BV, PO Box 99, 4000 AB Tiel, The Netherlands, bioMérieux BV, Boseind 15, 5281 RM Boxtel, The Netherlands, and LioniX BV, PO Box 456, 7500 AH Enschede, The Netherlands

Received November 6, 2006; Revised Manuscript Received December 13, 2006

ABSTRACT

We report the application of an integrated optical Young interferometer sensor for ultrasensitive, real-time, direct detection of viruses. We have validated the sensor by detecting herpes simplex virus type 1 (HSV-1), but the principle is generally applicable. Detection of HSV-1 virus particles was performed by applying the virus sample onto a sensor surface coated with a specific antibody against HSV-1. The performance of the sensor was tested by monitoring virus samples at clinically relevant concentrations. We show that the Young interferometer sensor can specifically and sensitively detect HSV-1 at very low concentrations (850 particles/mL). We have further demonstrated that the sensor can specifically detect HSV-1 suspended in serum. Extrapolation of the results indicates that the sensitivity of the sensor approaches the detection of a single virus particle binding, yielding a sensor of unprecedented sensitivity with wide applications for viral diagnostics.

In recent years, there have been several examples of serious virus outbreaks such as severe acute respiratory syndrome (SARS) and H5N1 bird flu virus. There are significant fears that such outbreaks can rapidly spread worldwide to become pandemics with devastating effects on populations and their social and economic development. Therefore, fast, on-site, and sensitive detection of viruses is essential in detecting the onset of viral epidemics and preventing their spread. Traditional virus detection methods such as polymerase chain reaction (PCR)[1] and branched-chain DNA test (bDNA)[2] are not compatible with point-of-care settings as they are time-consuming, expensive, and require labor-intensive sample preparation. This has been the motivation behind the increased interest for the development of alternative virus detection methods reported in recent literature. One of them, called rupture event scanning technique,[3] is based on measurement of adhesion forces between a surface and virus particles. This technique is highly sensitive and can detect virus particles in complex samples such as serum; however, a lengthy preparation of antibody-coated surfaces (∼20 h) is required. Several other techniques[4−8] have demonstrated the feasibility for virus detection, but further investigation is required to show their utility in clinical settings and for the development of point-of-care systems. Here, we describe and test an alternative detection method that combines the different advantages of existing techniques in a single device. The device is extremely sensitive, compact (allows for point-of-care detection), easy to use, fast, and requires a minimal pretreatment of the sample. We believe that these properties make the current method extremely suitable in detecting, preventing, or controlling viral outbreaks.

We have recently developed a very sensitive antibody-based sensor for specific detection of, e.g., proteins. The sensor principle is based on a Young interferometer (YI) and requires no labeling of analyte molecules.[9] The sensitivity of 10^{-8} refractive index units, corresponding to approximately a protein mass coverage of 20 fg/mm^2, is among the most sensitive sensors reported.[10−12] This sensitivity is ∼2 orders of magnitude higher than other nonlabeling sensor techniques such as surface plasmon resonance.[13] Moreover, this sensor is simple, easy to use, and compact, offering the

* Corresponding author. E-mail: A.Ymeti@utwente.nl. Telephone: 0031534893870. Fax: 0031534891105.
† Biophysical Engineering, MESA+ Institute for Nanotechnology and Institute for Biomedical Technology.
‡ Integrated Optical Microsystems, MESA+ Institute for Nanotechnology.
§ Paradocs Group BV.
|| bioMérieux BV.
⊥ LioniX BV.
Deceased.

10.1021/nl062595n CCC: $37.00
Published on Web 12/29/2006

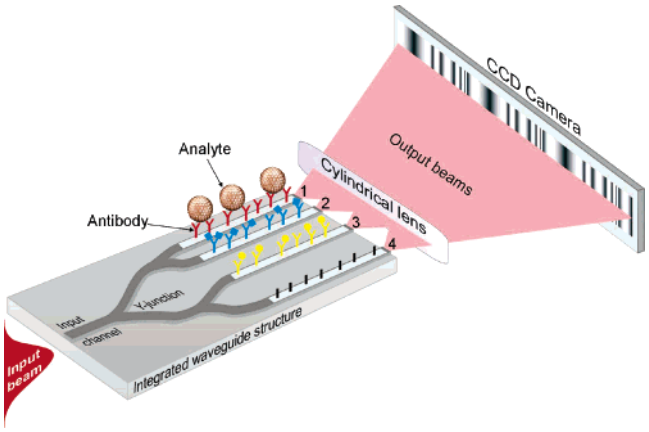

Figure 1. Representation of the sensor. Schematic of the four-channel integrated optical YI sensor (not on scale): **1**, **2**, and **3** indicate the measuring channels, and **4** is the reference channel.

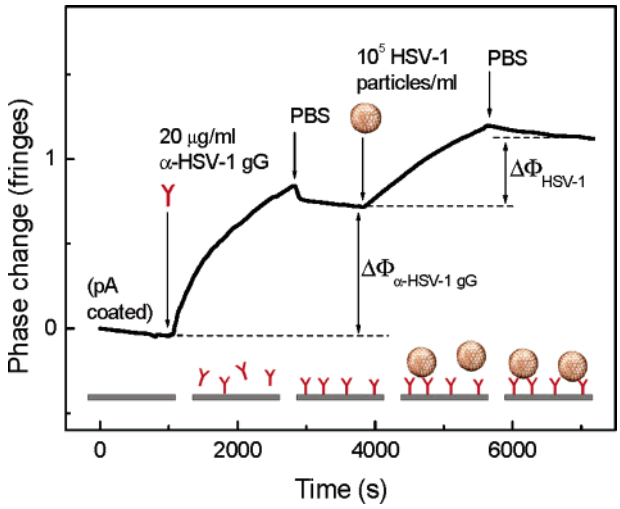

Figure 2. Virus detection test. Sensor signal (phase change) measured between channel 1 and the reference channel for the immobilization of anti-HSV-1 glycoprotein G monoclonal antibody layer on the sensing surface of channel 1 ($\Delta\Phi_{\alpha-\mathrm{HSV-1gG}}$) and the binding of HSV-1 particles to this layer ($\Delta\Phi_{\mathrm{HSV-1}}$).

possibility for development of portable point-of-care instruments. As such, this sensor is an excellent candidate for fast and on-site virus detection. Here we explore the use of this sensor for the detection of herpes simplex virus type 1. This virus causes recurrent mucosal infections of the eye, mouth, and genital tract. The detection principle of the sensor can be extended to any virus that has specific antibodies available such as human immunodeficiency virus (HIV), SARS, Hepatitis B and C, or even H5N1 bird flu virus. The multichannel character of the sensor allows sensing several (up to three in this configuration) different viruses and/or other pathogens simultaneously.

The principle of the sensor is schematically shown in Figure 1. Monochromatic light from a laser source is coupled to an optical channel waveguide and is guided into four parallel optical channels by means of Y-junctions. These four channels include one reference channel and up to three different measuring channels that can be used to monitor different analytes by coating the channels with appropriate antibodies. Upon exiting from these four waveguide channels, the light interferes on a screen, generating an interference pattern. Specific analyte binding to the antibody-coated waveguide surface, which is probed by the evanescent field of the guided modes, causes a corresponding phase change that is measured as a change in the interference pattern. Analysis of the interference pattern thus yields information on the amount of adsorbed analytes on different channels.

The feasibility of using the YI sensor for virus detection was explored by monitoring the interaction between anti-HSV-1 glycoprotein G monoclonal antibody (α-HSV-1gG) and HSV-1 virus particles (Virusys Corporation, Sykesville, MD, United States). Figure 2 shows the phase change measured between channel 1 and reference channel 4 in the four-channel YI sensor caused by the immobilization of a α-HSV-1gG layer on the sensing surface of channel 1, followed by the binding of HSV-1 virus particles to this layer. Here, a concentration of $\sim 10^5$ HSV-1 virus particles/mL was used. This test clearly demonstrates the detection of virus particles by the YI sensor.

Specificity of the YI sensor to HSV-1 was demonstrated by immobilizing different receptor layers in adjacent measuring channels and monitoring the sensor response to different analyte solutions. To do so, anti-human serum albumin (α-HSA; Sigma-Aldrich, St. Louis, MO) was immobilized in channel 1 by flowing a 200 μg/mL α-HSA solution prepared in phosphate buffered saline (PBS). In channel 2, α-HSV-1 gG was immobilized. Next, a solution of 50 μg/mL human serum albumin (HSA; Sigma-Aldrich, St. Louis, MO) in PBS was simultaneously applied in channels 1 and 2, and after approximately 30 min, flow was changed back to PBS for both channels. The observed binding curves are shown in Figure 3 (graphs A1 and A2, respectively). After achievement of a stable baseline, a 10^5 particles/mL HSV-1 solution was flowed in both channels (see B1 and B2 in Figure 3, respectively). The observation that a response is measured only for the α-HSA−HSA and α-HSV-1gG−HSV-1 interactions is a clear indication that the signals are caused by specific interactions and that cross reactivity between coatings is negligible.

To explore the dynamic range of the sensor and its sensitivity, the sensor was further tested with HSV-1 concentrations that varied from 8.5×10^2 to 8.5×10^6 particles/mL, covering the concentration range that corresponds to the classification "very low" to "very high" in terms of the viral load.[14] The phase changes that are observed at these viral concentrations are plotted in Figure 4A and demonstrate a dynamic range of at least 4 orders of magnitude. Figure S1 (see the Supporting Information) shows the excellent signal-to-noise ratio even for the lowest measured virus concentration.

Next, the sensor was tested using complex samples such as a virus suspended in serum. Figure 4B shows the response of the sensor after the application of a 10^5 HSV-1 particles/mL solution prepared in human serum in the sensing window of the measuring channel, which was previously coated with α-HSV-1gG. Note that we first added serum in the measuring channel. Later, virus-containing serum was added. According to Figure 4B, there is a clear response of the sensor due to

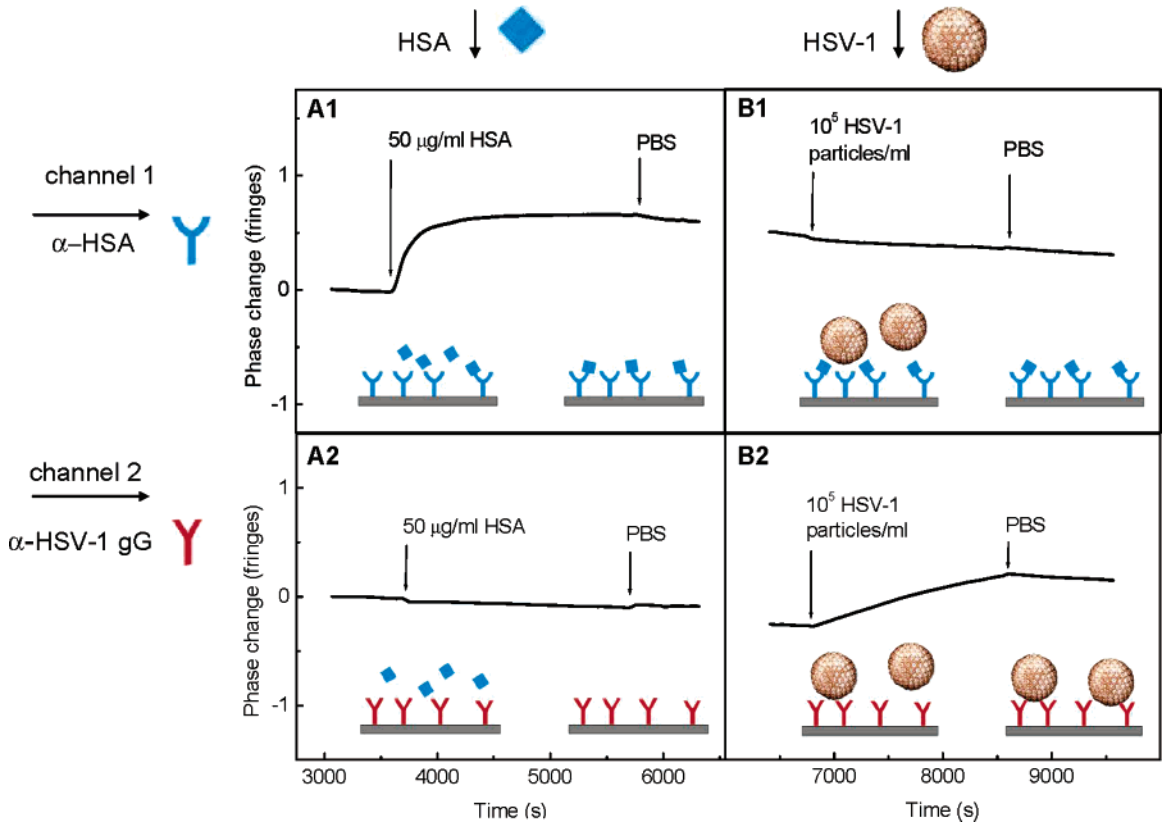

Figure 3. Specific detection of HSV-1. Phase changes $\Delta\Phi_{14}$ and $\Delta\Phi_{24}$ in the four-channel YI sensor as a function of time during several processes. HSA solution was first flowed through channels 1 and 2 simultaneously (A1 and A2). Next, after washing with PBS, HSV-1 solution was flowed in channels 1 and 2 simultaneously (B1 and B2); PBS was continuously flowed in reference channel 4. Thus, the four graphs show the following interactions: (A1) α-HSA−HSA, (A2) α-HSV-1gG−HSA, (B1) α-HSA−HSV-1, (B2) α-HSV-1gG−HSV-1. Note that initial phases in A1 and A2 were shifted to 0 for clarity.

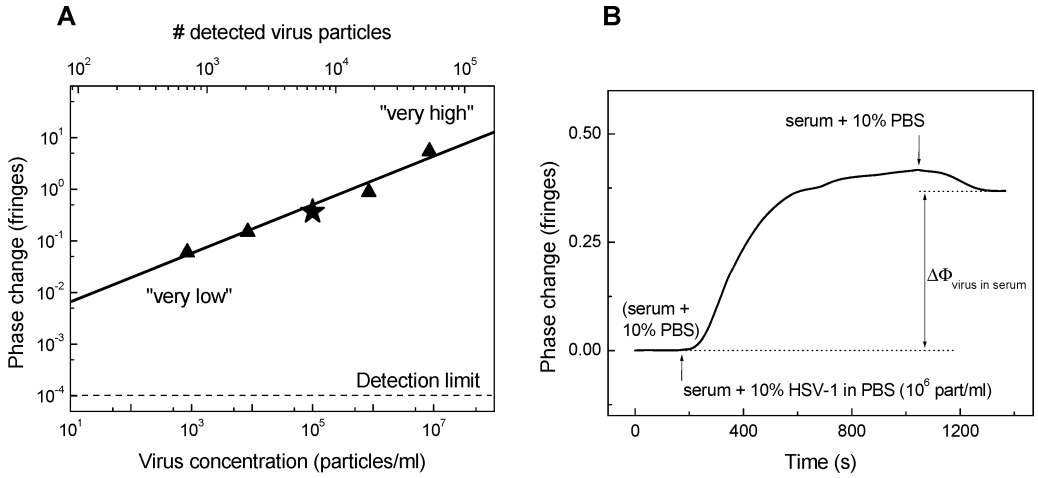

Figure 4. Measurement of different HSV-1 concentrations and detection in serum. (A) Phase change measured for different concentrations of HSV-1 sample solutions in PBS applied in the measuring channel of the YI sensor (▲). Solid line is a linear-fit of the experimental data, (★) represents the phase change measured for HSV-1 diluted in serum (see Figure 4B), dashed line indicates the phase detection limit of the sensor. (B) Sensor response due to the binding of HSV-1 diluted in serum. Final concentration of HSV-1 was 10^5 particles/mL. The total signal is estimated to be $\Delta\Phi_{\text{virus in serum}} = 0.37$ fringes, consistent with results obtained in PBS (see ★ in Figure 4A).

the binding of HSV-1 and is in good agreement with the measurement of HSV-1 in buffer, as indicated in Figure 4A. To confirm the specificity of HSV-1−α-HSV-1gG interaction, we carried out a control experiment in which no antibody was immobilized in the measuring channel. No response was measured when the virus solution in serum was applied (graph not shown), indicating the specificity of HSV-1−α-HSV-1gG interaction.

The results obtained clearly demonstrate the feasibility to specifically detect capture of virus particles using an

integrated optical Young interferometer-based sensor. Moreover, it demonstrates the possibility to detect such binding at very low particle concentrations and at a low number of virus particles.

In the measured, clinically relevant concentration range,[14] covering 4 orders of magnitude, a clear relation between the sensor signal and the viral concentration is found (a linear fit through the data points in Figure 4A gives a correlation coefficient of 0.98) that allows virus concentration predictions given a calibrated sensor. Given the high signal-to-noise ratio of 2×10^2 (at a bandwidth of 0.1 Hz) that was observed at the lowest virus concentration (850 particles/mL), it is likely that much lower concentrations can be detected with the current sensor. An estimation of the number of captured HSV-1 particles can be made given the size (150−200 nm)[15] and the refractive index (∼1.41).[16] This results in a phase change of $\sim 1.1 \times 10^{-4}$ fringes for the binding of a single virus particle (see the Supporting Information). This means that, for the lowest measured concentration (see Figure S1 in the Supporting Information), during the course of the measurements, ∼700 virus particles were detected with an average binding rate of 1 virus every 4 s. From these estimations, it can be argued that the detection limit of the sensor (10^{-4} fringes) can approach that of a single HSV-1 particle binding.

From Figure 3, we conclude that, by using specific antibody coatings of the different channels, it is possible to specifically detect various analytes in parallel. This applies both for virus particles as well as for antigens. Very importantly, the YI sensor allows specific detection of virus particles suspended in serum. Although there is a background due to nonspecific binding of serum proteins, the signal due to binding of virus particles could be easily detected. This lends credence to the use of this type of sensor for clinical applications. Although the background remains a drawback of this approach, the influence of the background can be considerably reduced by using differential phase change information from different measuring channels. Moreover, attention should be paid to improvement of the measuring channels coating, which should result in a further reduction of the background.

Using the results achieved here, we can compare this sensor to the standard methods for virus detection. The sensitivity of this sensor is comparable to the most sensitive methods reported so far such as PCR,[1] bDNA,[2] and the more recently developed methods such as the rupture event scanning technique.[3] However, these methods are rather time-consuming and/or labor-intensive and therefore less suitable for point-of-care application. Although the measurements presented here show that it takes approximately 1 h for the virus to bind to the sensor surface, it is possible to estimate the concentration of the applied virus suspension by only measuring the response of the sensor in the first few minutes (a correlation coefficient of 0.95 was found between the virus concentration and the measured slope, see Figure S2 in the Supporting Information). Especially in combination with microfluidics, as demonstrated in ref 17, the YI sensor requires small sample volumes (∼μL) and shows a short-time response (∼s). A miniaturized stand-alone prototype of this sensor is currently under development.

Considering the extremely high sensitivity, the short-time response, multiplexing capability, and the prospect to develop the sensor as a robust handheld device using disposable precoated sensor chips, it is anticipated that the Young interferometer-based virus sensor is a strong candidate for a point-of-care viral diagnostics.

Acknowledgment. This project was financially supported by the Dutch Technology Foundation STW (grant no. TTN.4446). This article is dedicated to Stephan W.F.M. van Hövell.

Supporting Information Available: Additional figures showing measurement of the lowest virus concentration, fast estimation of virus concentrations, and a photograph of the sensor; estimation of phase change of the captured virus particles, and experimental section. This material is available free of charge via the Internet at http://pubs.acs.org.

References

(1) Piatak, M.; Saag, M. S.; Yang, L. C.; Clark, S. J.; Kappes, J. C.; Luk, K. C.; Hahn, B. H.; Shaw, G. M.; Lifson, J. D. *Science* **1993**, *259*, 1749−1754.
(2) Pachl, C.; Todd, J. A.; Kern, D. G.; Sheridan, P. J.; Fong, S. J.; Stempien, M.; Hoo, B.; Besemer, D.; Yeghiazarian, T.; Irvine, B.; Kolberg, J.; Kokka, R.; Neuwald, P.; Urdea, M. S. *J. Acquired Immune Defic. Syndr. Hum. Retrovirol.* **1995**, *8*, 446−454.
(3) Cooper, M. A.; Dultsev, F. N.; Minson, T.; Ostanin, V. P.; Abell, C.; Klenerman, D. *Nat. Biotechnol.* **2001**, *19*, 833−837.
(4) Patolsky, F.; Zheng, G. F.; Hayden, O.; Lakadamyali, M.; Zhuang, X. W.; Lieber, C. M. *Proc. Natl. Acad. Sci. U.S.A.* **2004**, *101*, 14017−14022.
(5) Gupta, A.; Akin, D.; Bashir, R. *Appl. Phys. Lett.* **2004**, *84*, 1976−1978.
(6) Ilic, B.; Yang, Y.; Craighead, H. G. *Appl. Phys. Lett.* **2004**, *85*, 2604−2606.
(7) Zaytseva, N. V.; Montagna, R. A.; Baeumner, A. J. *Anal. Chem.* **2005**, *77*, 7520−7527.
(8) Ignatovich, F. V.; Novotny, L. *Phys. Rev. Lett.* **2006**, *96*, 013901.
(9) Ymeti, A.; Kanger, J. S.; Greve, J.; Lambeck, P. V.; Wijn, R.; Heideman, R. G. *Appl. Opt.* **2003**, *42*, 5649−5660.
(10) Heideman, R. G.; Lambeck, P. V. *Sens. Actuators, B* **1999**, *61*, 100−127.
(11) Brandenburg, A. *Sens. Actuators, B* **1997**, *39*, 266−271.
(12) Cross, G. H.; Reeves, A. A.; Brand, S.; Popplewell, J. F.; Peel, L. L.; Swann, M. J.; Freeman, N. J. *Biosens. Bioelectron.* **2003**, *19*, 383−390.
(13) Berger, C. E. H.; Beumer, T. A. M.; Kooyman, R. P. H.; Greve, J. *Anal. Chem.* **1998**, *70*, 703−706.
(14) Mellors, J. W.; Rinaldo, C. R.; Gupta, P.; White, R. M.; Todd, J. A.; Kingsley, L. A. *Science* **1996**, *272*, 1167−1170.
(15) Levine, A. J. *Viruses*; Scientific American Library: New York, 1992.
(16) Balch, W. M.; Vaughn, J.; Novotny, J.; Drapeau, D. T.; Vaillancourt, R.; Lapierre, J.; Ashe, A. *Limnol. Oceanogr.* **2000**, *45*, 492−498.
(17) Ymeti, A.; Kanger, J. S.; Greve, J.; Besselink, G. A. J.; Lambeck, P. V.; Wijn, R.; Heideman, R. G. *Biosens. Bioelectron.* **2005**, *20*, 1417−1421.

NL062595N